Journal of Chromatography, 559 (1991) 183–196
Elsevier Science Publishers B.V., Amsterdam

CHROM. 23 632

Laser-induced fluorescence and fluorescence microscopy for capillary electrophoresis zone detection[a]

LUIS HERNANDEZ*[,b] and JOSE ESCALONA
Laboratory of Behavioral Physiology, School of Medicine, Los Andes University, Merida 5101-A (Venezuela)
NARAHARI JOSHI
Center for Advanced Optic Studies, Physics Department, Los Andes University, Merida 5101-A (Venezuela)
and
NORBERTO GUZMAN[c]
Princeton Biochemicals Inc., Princeton, NJ 08543 (USA)

ABSTRACT

A procedure to improve on-column fluorescence detection for capillary zone electrophoresis is reported. A fluorescence detector was built using an epillumination fluorescence microscope and an argon-ion air-cooled laser. The 488-nm line was isolated with a band pass filter to eliminate the ultraviolet line. A dichroic mirror which reflected wavelengths under 510 nm and a 0.75 numerical aperture (NA), 0.3 mm working distance objective of the microscope condensed the laser beam on a fused-silica capillary and a cross-shaped fluorescence spot was observed. The emitted light was collected with the same objective, filtered with a 520-nm high pass filter, a spatial filter and a notch filter, and focused on a photodetector. The photodetector was either a gallium–arsenide or a multialkali photomultiplier tube. The signal generated was fed to a current-to-voltage converter and registered on a strip chart recorder. The detector was tested with fluorescein-derivatized amino acids. For the fluorescein thiocarbamyl (FTC)-amino acids the limit of concentration detection varied according to the amino acid. Taking FTC-arginine as the best example, the limit of concentration detection (LOCD) was $3.75 \cdot 10^{-12}$ *M*. Assuming that 1 nl was injcted, the limit of mass detection (LOMD) was $3.75 \cdot 10^{-3}$ amol or about 2250 molecules. This represents an improvement of about three orders of magnitude with respect to previous laser induced fluorescence on-column detection. The potential and advantages when using an epillumination fluorescence microscope with laser induced fluorescence as a detection system for capillary electrophoresis are discussed.

INTRODUCTION

Since Gassman *et al.* [1] introduced laser induced fluorescence detection (LIFD) for capillary electrophoresis (CE), LIFD has gradually become the most sensitive technique for analyte detection in narrow bore capillaries. With the 325-nm line of the

[a] Part of this work was presented at the *2nd International Symposium on High Performance Capillary Electrophoresis, San Francisco, CA, January 29–31, 1990.*

[b] Address for correspondence: Europhor SA, Parc Technologique du Canal, 10 Avenue de l'Europe, 31520 Ramonville, Toulouse, France.

[c] Present address: Pharmaceutical Research and Development, Hoffmann-La Roche Inc., 340 Kingsland Street, Nutley, NJ 07110-1199, USA.

0021-9673/91/$03.50

He–Cd laser, dansylated derivatives of amino acids, vitamins, and drugs have been detected on-column [1–5]. The limit of concentration detection (LOCD) for some dansylated amino acids was about 10^{-9} *M* and the limit of mass detection (LOMD) was about 10 amol. For some drugs such as metrotexate the LOCD was 10^{-10} *M*. The same type of laser has been used for indirect fluorescence detection to analyze non-fluorescent and non-derivatizable compounds, in the same on-column detection mode [6–9]. When applying the indirect fluorescence detection system the LOCD was about 10^{-6} *M* and the LOMD was approximately 1 fmol, using 50 μm I.D. capillaries.

When using the 442-nm line of the He–Cd laser and fluorescein isothiocyanate (FITC) as derivatizing agent, the LOCD for phenylalanine was close to 10^{-10} *M* and the LOMD about 1 amol. For other derivatized amino acids such as glutamic acid, the LOCD was 10^{-7} *M* [10]. In these experiments an excess of amino acids with respect to FITC was used. The LOCD was calculated on the basis of the fluorescein thiocarbamyl (FTC)-amino acid concentration assuming full reaction of the FITC. In the same report, with the 325-nm line and the 420-nm line of the He–Cd laser, and for ortho-phthalaldehyde (OPA) and naphthalenedialdehyde (NDA) derivatized amino acids, the LOCD was 10^{-8} *M* and 10^{-9} *M*, respectively. These values represent the highest sensitivities for amino acids in the on-column detection mode. The He–Cd laser has also been used to detect rapidly separated dansylated or OPA-derivatized amino acids in 10 μm I.D. capillaries [11]. In these experiments a mixture of eight amino acids was resolved in less than 90 s, but the LOCD was reduced by one order of magnitude due to the smaller diameter of the capillary. Other laser-based detection methods such as fluorescence detected circular dichroism [12], thermooptical absorbance detection [13], refractive index detection [14], and refractive index and absorbance detection [15] have been used, but the sensitivity values reported were lower than for LIFD.

A recent breakthrough was the use of the 488-nm wavelength line of an argon-ion laser for the detection of fluorescein isothiocyanate-derivatized amino acids separated by CE in 50 μm I.D. capillaries with a post-column detection mode [16]. Detection was carried out on a quartz sheath-flow cuvette at the cathodic end of the capillary. Again, the concentration of tagged amino acid was calculated assuming full reaction of FITC with an excess of amino acid. Subattomole amounts of FTC-amino acids were measured; in the case of arginine, the LOCD was 10^{-12} *M* [17]. This concentration value represents the highest sensitivity ever reached for CE. Therefore, 10^{-9} *M* seems to be the best LOCD for on-column detection, and 10^{-12} *M* for post-column detection.

There are many applications in which post-column detection is used. However, on-column detection may be required in many other applications of CE, such as in the case of DNA sequencing. In this application CE and LIFD have proved to be an excellent method for rapid separation and detection of fluorescein-derivatized fragments of DNA using gel-filled capillaries [18–20]. The LOCD for a fluorescein primer was about 10^{-11} *M* in 50 μm I.D. and 75 μm I.D. capillaries. In these experiments, the fluorescein primer was not electrophoretically migrated through the capillary. A vacuum pump was used to flush the capillary continuously with the fluorescein solution. Under these circumstances, photobleaching is minimized and the LOCD is better than in electromigration. When the primer was injected in a gel-filled capillary [20], the LOCD was $1.5 \cdot 10^{-10}$ *M*. Recently, a successful attempt to put together the sheath-flow cuvette method and DNA separation in gel-filed capillaries

was conducted [21]. Subattomole amounts of FITC-labelled DNA fragments were measured. But it seems that the procedure does not allow detection from several capillaries in a single run. This represents a disadvantage because to make CE DNA sequencing competitive with slab gel DNA sequencing, multiple capillaries will have to be used simultaneously. This technical problem may be solved in the near future, but in any event improvement in sensitivity for on-column LIFD in capillaries of 50 μm I.D. or less remains a necessity for both DNA sequencing and amino acid analysis by CE-LIFD.

In all these instruments the direction of the excitation radiation is orthogonal with the emitted radiation. Glass or quartz lenses or fiber optics have been used to focus the laser on the capillary and to focus the emitted radiation on the light sensitive element. However, the orthogonal design makes it hard to use lenses of very small working distance and, as a consequence, limits the numerical aperture (NA) of the lenses to about 0.45. Fiber optics solve the alignment difficulties inherent to the lenses and the fiber can collect very close to the capillary. However, the feeble fluorescent signals are attenuated by internal scattering in the fiber.

In a previous report [22] we examined the advantages of the collinear arrangement when using an epillumination fluorescence microscope as an alternative to the orthogonal arrangement for the on-column detection in CE. Using a mercury lamp as the excitation source, a quadratic relationship was found between the numerical aperture or magnification of the microscope lenses and the intensity of the fluorescence. Maximum signals were obtained with high magnification, high numerical aperture lenses that had a working distance of less than 1 mm. At the present time, the collinear arrangement has not been used in LIFD for CE, and therefore the advantages of lenses of high numerical aperture have not been fully exploited. The combination of an epillumination fluorescence microscope and a coherent source of excitation radiation may improve LIFD in several ways. (1) Focusing the laser on the capillary could be easy because the microscope already has a highly precise *XYZ* displacement device, and the alignment of the capillary can be guided visually. (2) The excitation of the sample and the detection of the emitted light would be done on the same side of the capillary (collinear arrangement). For the majority of phonon symmetries, Raman scattering efficiencies are nearly maximum perpendicular to the plane of symmetry and therefore the directions of incident and scattered light are generally at right angles to each other [23,24]. Then, the orientation of the sample is adjusted relative to the incident beam to achieve maximum response (this angle very often lies between 37 and 42°). Contribution of Raman scattering originating from prominent vibrational modes is avoided completely in the back scattering geometry. (3) The emitted light could be collected with lenses of less than 1 mm working distance and higher numerical aperture than the lenses that have been used so far in the orthogonal arrangement for the purpose of enhancing the fluorescent signal. (4) The emitted light could easily be focused on the photodetector because the microscope already has the optics for that task.

We now report this application and an improvement of at least 3 orders of magnitude in LOCD for the on-column detection of FTC-amino acids.

EXPERIMENTAL

Instrumentation

A diagram of the instrument is shown in Fig. 1. The microscope as a Model Standard 14 IFD Zeiss epillumination fluorescence microscope. It was equipped with heat suppression and interference filters. The laser was a Model 161-C Spectraphysics, 488-nm, argon-ion, air-cooled laser, kindly donated by Europhor SA (Toulouse, France). This laser was placed behind the microscope on a jack. The beam of coherent light was filtered through a 450–490 nm filter band pass (Model BP 450-490, Carl Zeiss, Oberkochen, Germany), reflected by a 510-nm chromatic beam splitter (Model FT-510, Carl Zeiss) and condensed on the capillary by means of a fluorite objective (Model Neofluar, Carl Zeiss). The emitted light was collected by the same objective. After crossing the chromatic beam splitter, it was filtered through a 520-nm long wave pass filter (Model LP-520, Carl Zeiss), a home made spatial filter, and a custom made notch filter centered at 492 nm, with a bandwidth of 33 nm and 90% transmittance at 530 nm (kindly donated by Andover Corp., Salem, NH, USA). This last one sup-

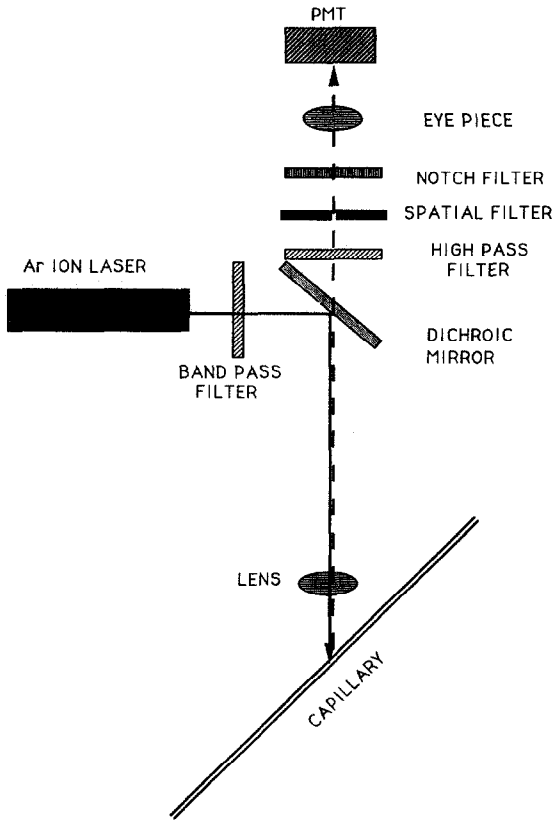

Fig. 1. Diagram of a collinear laser-induced fluorescence detection system. The data of the objectives are tabulated in Table I. The main axis of the capillary is at a 90° angle with the laser beam and with the optical axis of the microscope. The ocular is a 10× glass lens, the spatial filter either 2 or 3 mm diameter.

pressed the 488-nm line that the capillary reflected toward the photodetector; even though specular reflection was high, it was well suppressed by the notch filter. A glass 10 × ocular was placed between the notch filter and the detector to focus the fluorescence on one of the following components. For one experiment the fluorescence was focused on the monochromator of a SPEX spectral analyzer equipped with a water-cooled cathode, galium–arsenide Model 60-ER Hamamatsu tube operated at 2000 V (SPEX Industries, Edison, NJ, USA). For the other experiments the signal was focused on the quartz window of a multialkali Model R928 Hamamatsu photomultiplier tube (PMT) (Hamamatsu, Bridgewater, NJ, USA), operated at 750 V with a Model 215 Bertan high-voltage power supply (Bertan, Hicksville, NY, USA). The output of the Ga–As PMT was connected to a photon counting module and to a dedicated computer for statistical processing. The output of the multialkali PMT was connected to a Model 485 Keithley picoammeter (Keithley, Cleveland, OH, USA) operated at 200 nA for weak signals. Photographs were made with an automatic camera (Model M-63, Carl Zeiss), and the signal was recorded on a strip chart recorder (Model L-6512, Linseis, Princeton Junction, NJ, USA). A special capillary carrier described elsewhere was used [22]. To diminish light scattering and reduce background noise a hole was drilled in the capillary carrier. The laser went through the hole and was absorbed by a black cylinder underneath the hole. The capillaries used were fused-silica, 90 cm long (Polymicro Technologies, Phoenix, AZ, USA). The I.D. of the capillaries varied between 5 and 75 μm and the O.D. between 140 and 144 μm. The polyimide cover of the capillary was burned away on a 0.5-cm segment at 60 cm from the injection end, and the capillary was positioned in the capillary carrier and set on the stage of the microscope. The two ends of the capillary were immersed in a 40 m*M* carbonate buffer solution at pH 10.0. The capillary was primed by means of a vacuum pump. The driving force to load and run the samples was provided by a Model prime vision V Europhor high-voltage power supply (Europhor) in the constant voltage mode.

Laser and capillary alignment. The laser was easily aligned with the capillary because the microscope has a feature to simplify this operation. A reticule on one ocular indicated where the center of the visual field was. With the leveled jack the laser could be raised and lowered. The lateral movements were done by hand. Since the microscope is equipped with binoculars to watch the object, it was an entirely visually guided operation. The capillary was filled with a fluorescent solution (for example 10^{-10} *M* derivatized glycine) to facilitate alignment. The capillary was displaced with the *XY* displacement mechanism of the stage. The capillary and the laser were displaced until they coincide with the reticule. The entire operation lasted about two minutes. Once the laser and the capillary were centered, the *Z* displacement was used to produce a sharp image of the capillary. When the PMT is properly set, the image of the fluorescent spot is focused on the light sensitive window.

Reagents

Sodium carbonate, sodium bicarbonate, arginine, glycine, cysteine, isoleucine, leucine, methionine, alanine and fluorescein isothiocyanate isomer I were purchased from Sigma (St. Louis, MO, USA). Acetone was obtained from Aldrich (Strasbourg, France).

Procedure

A $2.1 \cdot 10^{-4}$ *M* solution of fluorescein isothiocyanate (FITC) isomer I (Sigma) in acetone was prepared by dissolving 0.5 mg of FITC in 6 ml of acetone. Then, 2 mg of each amino acid were dissolved in 2 ml of 0.2 *M* carbonate buffer at pH 9.0. Of each amino acid solution 1 ml was allowed to react with 1 ml of the FITC solution for 4 h in the dark. At the same time, 1 ml of a $2.1 \cdot 10^{-4}$ *M* solution of FITC in acetone was mixed with 1 ml of 0.2 *M* carbonate buffer to obtain a blank and kept in darkness fo 4 h. Then, both the FITC solution and the amino acid plus FITC solution were diluted 10^8 times by steps of 10 in 0.05 *M* carbonate buffer at pH 10. The samples were electrokinetically loaded by immersing one end of the capillary and the positive electrode into the sample and applying 10 kV during 7.5 s. According to previous calculations of electroosmotic flow the injection volume is about 1 nl for 25 μm I.D. capillaries [22]. Then the end of the capillary and the positive electrode were transferred to a buffer reservoir and run at 20 kV. After each run the capillary was washed by sequential hydrodynamic injections of 1 *M* NaOH (2 min), 0.1 *M* NaOH (2 min), water (3 min) and buffer (4 min).

Several experiments were conducted to determine the optimum combination of numerical aperture, capillary diameter, and laser power in order to achieve the highest sensitivity. Then measurements of derivatized amino acids were performed.

In the first experiment 10^{-10} *M* FTC-leucine was injected into several capillaries and the signal was magnified with three different fluorite objectives. The data for the objectives are shown in Table I.

The fluorescent material was continually introduced by a vacuum pump. The laser power was 4 mW and the spatial filter was 2 mm diameter. The I.D.s of the capillaries were 5, 12, 15, 21, 29, 50 and 75 μm, and the O.D. varied between 140 and 144 μm. The best fitting curves for each NA were obtained from polynomial equations or from the linearized form of exponential equations [25]. The correlation coefficients were calculated for each curve. Pictures of the fluorescent spot were taken for the three objectives and without spatial filter on the 50 μm I.D. capillary. Then, with the 0.75 NA objective and the 10× ocular, three pictures were made of the image of the capillary, without spatial filter, with the 3-mm spatial filter and with the 2-mm spatial filter.

In the second experiment, the FTC-leucine solution signal and the background light of the capillary and the buffer were measured at ten different laser powers with 0.20, 0.40 and 0.75 NA objectives. In this experiment, the sample was continually introduced by vacuum in a 50 μm I.D., 140–144 μm O.D. capillary. No spatial filter was used and the ocular was 10×. The laser power was attenuated by regulating the

TABLE I

DATA OF THE OBJECTIVES USED IN EXPERIMENT 1

Magnification (×)	Numerical aperture	Working distance (mm)	Focal length (mm)
6.3	0.20	10.8	23.6
16.0	0.40	0.9	10.8
40.0	0.75	0.33	4.5

current. The laser power at the exit of the laser was read on the remote control unit of the laser. Regression analysis was used to calculate the slopes of the best-fitting curves. In this experiment samples of the PMT current fluctuations due to the capillary and the buffer were measured 20 times at each laser power during bouts of 5 s. The standard deviation of this fluctuations was calculated and the noise estimated as three times the standard deviation. A comparison with the root mean square of the peak-to-peak measurements of the noise gave the same noise level as the 3σ method.

In the third experiment a spectral analysis of 10^{-11} *M* fluorescein-labelled isoleucin was performed. A 25 μm I.D. capillary and a 40 ×, 0.75 NA fluorite objective combined with a 10 × ocular and a 2-mm spatial filter were used. The capillary was continually flushed with the fluorescent solution by means of a vacuum pump. The fluorescence spot was fed into a spectrum analyzer (SPEX) and processed by a computer driven monochromator. Because of the low intensity of radiation, the largest slit widths (1.2-mm entrance and 0.8-mm exit) were used. In this way, radiation detection capability was increased at the expense of spectral resolution. The 60-ER has a flat response in the entire range and, therefore, detector correction was not needed.

In the fourth experiment the tagged amino acids (10^{-6}, 10^{-7}, 10^{-8}, 10^{-9}, 10^{-10} and 10^{-11} *M* solutions) were loaded in a 25-μm capillary and analyzed to determine the LOCD, the LOMD and the linearity of the analysis. The laser power was kept at 4 mW and a spatial filter of 2 mm diameter was used. Each amino acid was run individually at the above-mentioned concentrations. The PMT current produced by the peak of the FTC-amino acid was recorded and the baseline subtracted from the fluorescent signal. Then the log of the FTC-amino acid concentration *vs.* the log of the PMT current were plotted. A linear regression analysis was carried out to establish the dynamic range of the instrument. Then a mixture of six amino acids was prepared and run under the same conditions as for the individual FTC-amino acids.

RESULTS

The results of the first experiment are shown in Figs. 2, 3, 4 and 5. The three curves in Fig. 2 correspond to the three fluorite objectives. For the 0.20 NA objective, an increase of signal of 50 nA was observed between the 50 μm I.D. and the 75 μm I.D. capillaries. For the 0.40 NA objective, the largest increase of signal (86 nA) was observed between the 15 μm I.D. and 20 μm I.D. capillaries. The best signals were obtained with the 0.75 NA objective. The largest increase of signal (178 nA) was observed between the 5 μm I.D. and the 12 μm I.D. capillaries.

The pictures of the fluorescent spot are shown in Figs. 3 and 4. First of all, the size of the fluorescent spot increases as the numerical aperture of the objective increases. Comparing the surface of the spots in Fig. 3, the sizes for the three spots are: 0.20 NA, 24 mm^2; 0.40 NA, 96 mm^2; and 0.75 NA, 380 mm^2. In other words: the size of the fluorescent spot for the 0.75 NA objective is four times and fifteen times larger than the size of the fluorescent spots for the 0.40 NA and 0.20 NA objectives, respectively. When the surface of the spots were normalized to the surface of the spot seen with the 0.20 NA lens, the relative surface of the spot (1, 4 and 15) for the three objectives increased linearly with the collection efficiency of the objectives (1, 4 and 18%). Second, the three spots also differed in shape. For the 0.20 NA objective the spot is rectangular with the largest arista oriented in the same direction as the main axis of the

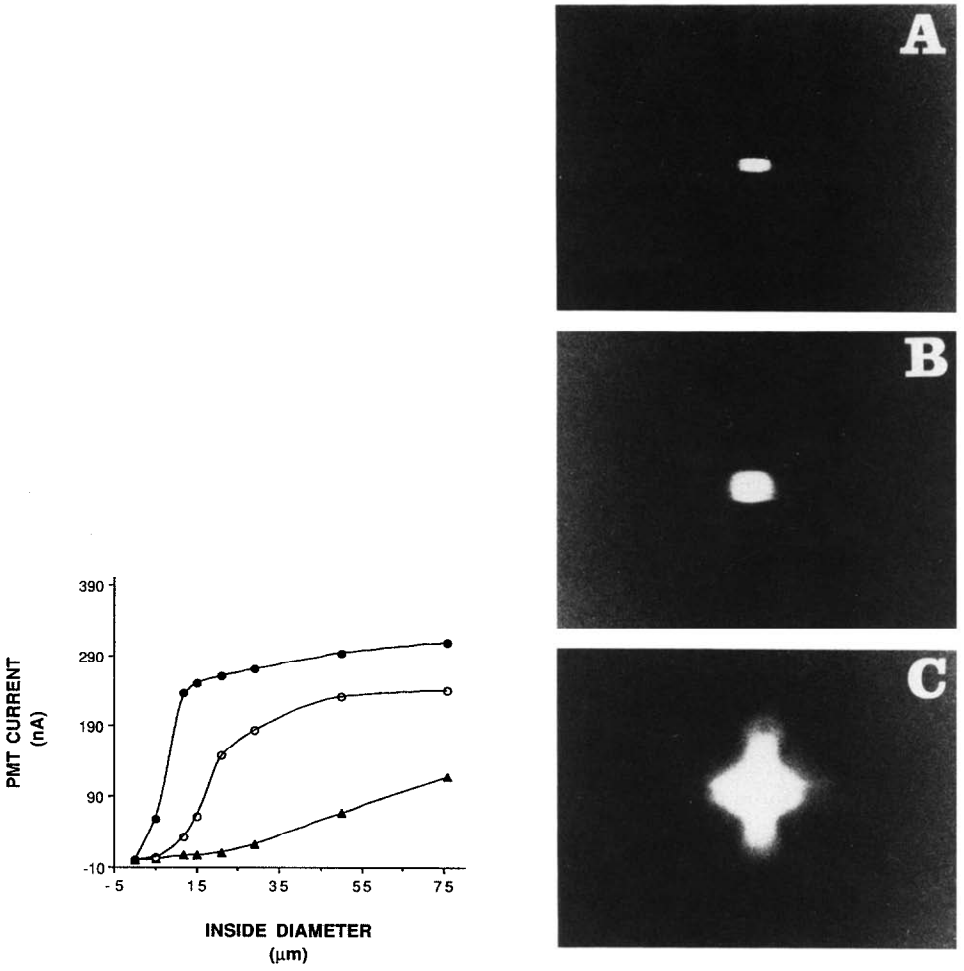

Fig. 2. Magnitude of a fluorescent signal as a function of the I.D. of the capillary and the numerical aperture of the objective. ● = 0.75 NA; ○ = 0.40 NA; ▲ = 0.20 NA. Notice the sharp rise of the intensity of the signal between the 5-μm and the 12-μm capillaries in the 0.75 NA curve.

Fig. 3. Microphotographs of the fluorescence with three objectives of different numerical aperture. (A) 0.20 NA, (B) 0.40 NA, (C) 0.75 NA. The size of th spot increases and the shape changes as the numerical aperture of the objectives increases. The 0.75 NA objective captures fluorescence emitted orthogonal as well as parallel to the main axis of the capillary. By contrast, the 0.20 NA and the 0.40 NA objectives capture only the fluorescence emitted parallel to the main axis of the capillary.

capillary. This shape is preserved by the 0.40 NA objective, but for the 0.75 NA objective the spot looks like a cross. Although it cannot be appreciated in these black-and-white reproductions, the cross is surrounded by a yellow halo that is produced by the walls of the capillary. The insertion of a spatial filter between the long wave pass filter and the notch filter reduces the size of the spot and suppresses the yellow halo (Fig. 4). At the same time there is a reduction of fluorescent intensity that can be compensated by raising the power of the laser.

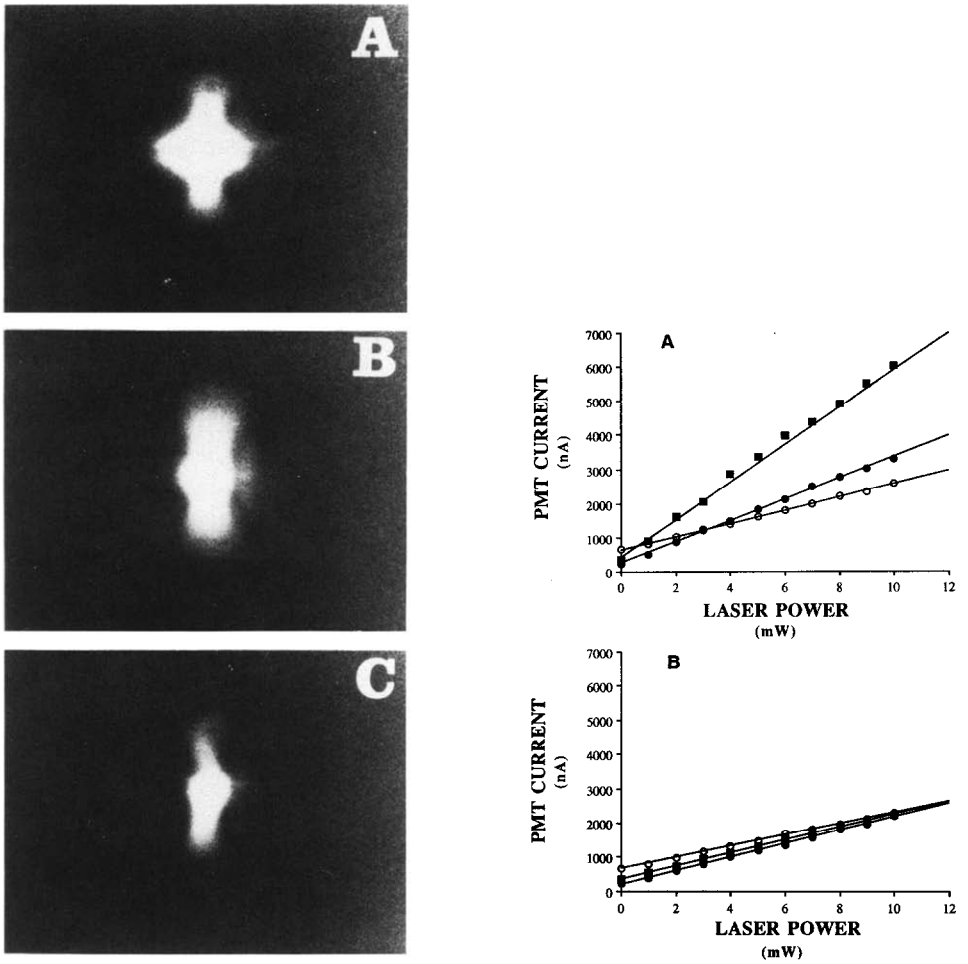

Fig. 4. Microphotographs showing the effects of spatial filters. (A) Unfiltered signal; (B) filtered through a 3 mm diameter spatial filter; (C) filtered through a 2 mm diameter spatial filter.

Fig. 5. Relationship between the laser power, the fluorescence and the numerical aperture of the objective. (A) Shows the fluorescence (in terms of PMT current) of a 10^{-10} *M* FTC-leucine solution *vs.* the laser power. Three objectives were tested: ■ = 0.75 NA, ● = 0.40 NA, ○ = 0.20 NA. The slope of the curves increases as a function of numerical aperture. (B) Shows the same relation but for a buffer filled capillary. No change of slope was observed as the numerical aperture of the objectives increased.

The increase of the laser power between 0 and 10 mW also increases the background light due to the capillary and the buffer, as shown in Fig. 5. However, the increase of numerical aperture increases the slope of the laser power *vs.* fluorescence curve only when a fluorescent solution is present into the capillary. As can be observed in Fig. 5, the slope of the curve generated by the 0.75 NA lens was 570, for the 0.40 NA the slope was 313.5 and for the 0.20 NA it was 193.7. This increase of signal due to the increase of numerical aperture is not observed when the buffer is filling the capillary. The bottom of Fig. 5 shows that the slopes of the equations for buffer-filled capillaries were 192, 198.5 and 166.5 for the 0.75, 0.40 and 0.20 NA objectives, respectively. The

fluctuations of the PMT current for the buffer were 1.76 ± 0.05 nA at any of the tested laser powers.

The result of the third experiment is shown in Fig. 6. The curve of fluorescent intensity rises from 515 nm and reaches a peak at 533 nm. Then it falls gradually to 585 nm. No peak is observed between 570 and 585 nm where the major Raman bands for water are located and detected in an orthogonal configuration.

Fig. 7 shows the electropherograms of six FTC-arginine solutions ranging from $2.1 \cdot 10^{-11}$ to $2.1 \cdot 10^{-6}$ *M* in steps of one order of magnitude. The top of the figure (electropherogram a) corresponds to the electropherogram of a $2.1 \cdot 10^{-11}$ *M* solution. The signal-to-noise ratio for this amount of FTC-arginine was 17:1. On this basis the LOCD was calculated to be a $3.75 \cdot 10^{-12}$ *M*. Since the signal was generated by an injection volume of 1 nl, the LOMD was $3.7 \cdot 10^{-3}$ amol or 2250 molecules. Fig. 7 also shows the log–log plot of concentration *vs.* signal intensity. This relationship was linear as demonstrated by the high correlation coefficient. The insets of Fig. 7 show the small margin of variation of the actual electropherograms, particularly between $2.1 \cdot 10^{-11}$ and $2.1 \cdot 10^{-7}$ *M* FTC-arginine concentrations. A large decrease of signal is observed at $2.1 \cdot 10^{-6}$ *M* (electropherogram f). However, the linearity of the measurements had a high correlation coefficient even when the data of the $2.1 \cdot 10^{-6}$ *M* solution were included in the analysis. For the detailed description of Fig. 7, please see the figure legend.

The result of the analysis of a mixture of six amino acids is shown in Fig. 8. The order of elution was arginine, leucine, methionine, cysteine, alanine and glycine. The concentration of FTC-amino acid was $2.1 \cdot 10^{-9}$ *M* for each. The peaks correspond to 2 amol in column. Arginine and glycine showed off-scale fluorescence, and cysteine showed the smallest signal. In addition, three blank peaks were observed. The largest

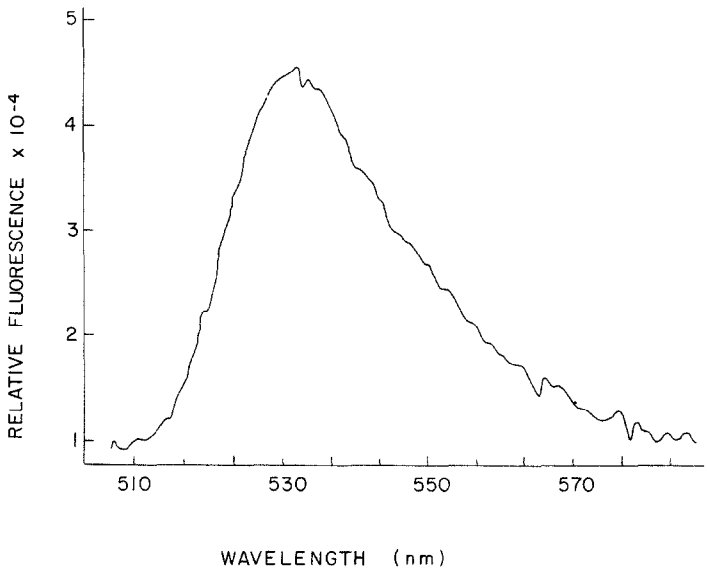

Fig. 6. Spectral analysis of a FTC-leucine solution. A peak is observed at 533 nm. No emission is observed between 560 and 580 nm.

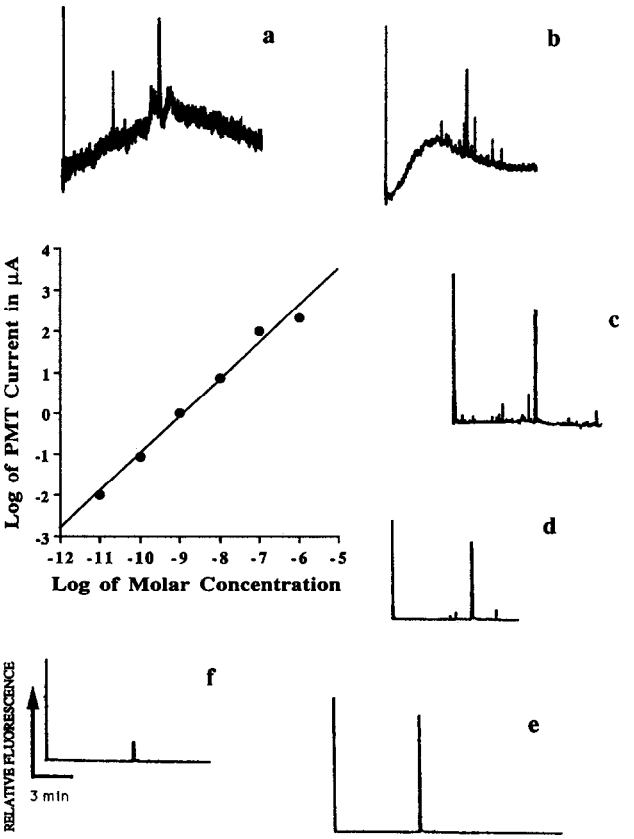

Fig. 7. Electropherograms of FTC-arginine solutions. The concentrations increased clockwise from a ($2.1 \cdot 10^{-11}$ *M*) to f ($2.1 \cdot 10^{-6}$ *M*) in steps of 10. The sensitivity of the instrument was decreased by steps of 10 from a to f. For example, the electropherogram c was generated at a sensitivity 1000 times lower than the electropherogram a. Between a and e the signals kept roughly the same height. Between e and f there is a decrease in signal height. The linearity of the instrument was analyzed by plotting the log of molar concentration *vs.* the log of the PMT current generated by the signal minus the baseline. Only between $2.1 \cdot 10^{-7}$ *M* and $2.1 \cdot 10^{-6}$ *M* was a deviation from linearity observed. The equation for this line was $y = 8.0 + 0.91x$ and the regression coefficient was $r = 0.98$.

one (peak 2) corresponds to unreacted fluorescein. Arginine and alanine had the trend to react fully with FITC. In their individual electropherograms no blank peaks were observed. By contrast, cysteine and glycine showed large peaks of unreacted FITC.

DISCUSSION

LIFD in a collinear arrangement allows on-column measurement of picomolar concentrations of FTC-amino acids in 25 μm I.D. capillaries. This represents an improvement of three orders of magnitude for laser-induced fluorescence on-column detection for CE. Several factors contribute to this sensitivity improvement. First, there is less Raman scattering due to the low volume of water in the detection cell, and

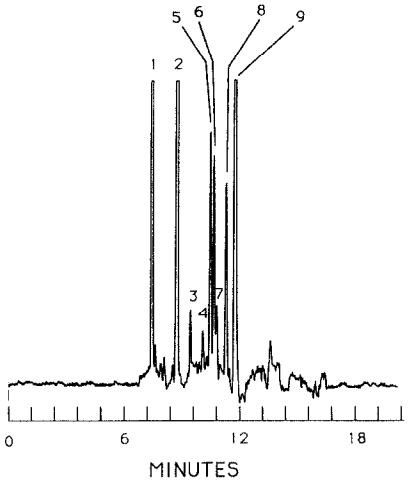

Fig. 8. Electropherogram of a mixture of six FTC-amino acids. The laser power was 4 mW, the spatial filter 2 mm diameter and the objective was the 0.75 NA one. The ocular was 10 ×. The analyte concentration was $2.1 \cdot 10^{-9}$ *M*, and the injection volume was 1 nl. The amount injected was 2.1 amol. Peaks: 1 = arginine; 2 = blank (probably unreacted FITC); 3 = blank; 4 = impurity of reagent; 5 = leucine; 6 = methionine; 7 = cysteine; 8 = alanine; 9 = glycine. FTC-arginine and FTC-glycine peaks were clipped.

due to the collinear collection of the fluorescence. The spectral analysis showed only the FITC emission band. No Raman bands were observed. Therefore, the background light was reduced and that allowed an increase in the current-to-voltage converter gain. Second, the collinear arrangement permits the use of higher numerical aperture lenses than those used in previous orthogonal instruments. This is an advantage because more fluorescence can be collected with large numerical aperture lenses. Fig. 3 shows that the largest numerical aperture gives the largest signal. In addition, Fig. 5 shows that the numerical aperture of the lenses is directly correlated with fluorescence collection but not with background radiation collection. In other words, the larger the numerical aperture of the lens, the larger the fluorescence, but this is not true for the background light produced by the capillary and the buffer. Therefore, the major source of noise in the instrument is scattered laser radiation, and not fluorescence of the capillary wall or the buffer. Third, the use of a notch filter to remove stray laser radiation decreases the background noise without significant decrease of the signal.

A 0.75 NA also allows work with narrow capillaries (between 12 and 15 μm I.D. capillaries) without a significant degradation of the LOCD due to smaller signal. Fig. 2 shows that there is a sharp drop in signal magnitude for the 0.40 NA lens when we pass from capillaries of 29 μm I.D. to 12 μm I.D. Such a drop was not observed with the 0.75 NA lens. This indicates that the instrument described here should perform with 12 μm I.D. capillaries nearly as well as with 25 μm I.D. capillaries. This feature can make it very useful for quick separation of amino acids by using the technique described by Nickerson and Jorgenson [10,11], with the advantage that the dynamic range will be extended to at least 10^{-11} *M* LOCD.

The collinear arrangement adds simplicity to the design of a laser-induced fluorescence detector. In fact, it eliminates the need for an optic bench. The instrument

of the present paper was assembled on a regular laboratory bench on a 40 × 50 cm area. This area is smaller than the one required to assemble orthogonal instruments. The alignment operation is also greatly simplified by the fact that it is visually guided with the microscope eyepieces and by means of a high quality *XY* displacer. Only one *XYZ* displacer is required in contrast with the orthogonal instruments in which at least two *XYZ* displacers are required. Moreover, orthogonal instruments require two optical systems, one for excitation and another for fluorescence collection. The present collinear instrument uses one optical system for both tasks. This helps to simplify the collinear instrument even further.

The linearity of the measurements extended over five orders of magnitude. Only at a very high concentration, $2.1 \cdot 10^{-6}$ *M* in the case of FTC-arginine, was deviation of linearity observed. Since this instrument is designed to work with rather small concentrations, the range of linearity of the instrument is satisfactory.

The sensitivity of this instrument still has considerable room for improvement. The dark current of the PMT operating in a dark room and with a shutter blocking all access of light to the tube, was about 200 pA with fluctuations of about 20 pA. The current generated by a picomolar solution was calculated to be about 6000 pA. It means that a picomolar solution can generate a signal 300 times larger than the dark current fluctuations of the PMT. However, the noise due to laser fluctuations was 1.76 nA, and the background current under our best conditions was about 90 nA. So the actual limiting factor for better sensitivity are the laser fluctuations. Nevertheless, the frequency of the laser fluctuations was about 1 Hz, and the minimal frequency of the unfilterad signal was 0.16 Hz. Therefore, with better electronic filtering, a noise reduction of at least one order of magnitude should be possible. This speculation indicates that, even though the sheath-flow cuvette technique still has the highest sensitivity for LIFD (the LOMD of the sheath-flow cuvette instrument is a few hundred molecules), in the near future, on-column detection with collinear arrangement could reach the sensitivity of post-column detection with the sheath-flow cuvette and orthogonal arrangement.

Another advantage of the collinear arrangement is that it simplifies the operation with multiple capillaries. Just by adding a motor-driven *XY* displacer it should be possible to change the excited capillary precisely. The technique of displacing an object by precise steps in the *XY* plane under the objective of a microscope is very well known in the field of microfluorometry. So it can be readily adapted to collinear LIFD with multiple capillaries. Currently, research is going on in this direction in our laboratories.

REFERENCES

1 E. Gassman, J. E. Kuo and R. Zare, *Science (Washington, D.C.)*, 230 (1985) 813.
2 D. Burton, M. J. Sepaniak and M. P. Maskarenik, *J. Chromatogr. Sci.*, 24 (1986) 347.
3 P. Gozel, E. Gassman, H. Michelsen and R. Zare, *Anal. Chem.*, 59 (1987) 44.
4 A. T. Balchunas and M. J. Sepaniak, *Anal. Chem.*, 59 (1987) 1466.
5 M. C. Roach, P. Gozel and R. Zare, *J. Chromatogr.*, 426 (1988) 129.
6 W. Kuhr and E. Yeung, *Anal. Chem.*, 60 (1988) 1832.
7 W. Kuhr and E. Yeung, *Anal. Chem.*, 60 (1988) 2642.
8 E. Yeung, *LC · GC*, 7 (1989) 118.
9 L. Gross and E. S. Yeung, *Anal. Chem.*, 62 (1990) 427.

10 B. Nickerson and J. W. Jorgenson, *J. High Resolut. Chromatogr.*, 11 (1988) 878.
11 B. Nickerson and J. W. Jorgenson, *J. High Resolut. Chromatogr.*, 11 (1988) 533.
12 P. L. Christensen and E. S. Yeung, *Anal. Chem.*, 61 (1989) 1344.
13 M. Yu and N. J. Dovichi, *Anal. Chem.*, 61 (1989) 37.
14 C.-Y. Chen, T. Demana, S. D. Huang and M. D. Morris, *Anal. Chem.*, 61 (1989) 1590.
15 D. J. Bornhop and N. J. Dovichi, *Anal. Chem.*, 59 (1987) 1632.
16 Y. F. Cheng and N. J. Dovichi, *Science (Washington, D.C.)*, 242 (1988) 562.
17 S. Wu and N. J. Dovichi, *J. Chromatogr.*, 480 (1989) 141.
18 H. Drossman, J. A. Luckey, A. J. Kostichka, J. D'Cunha and L. M. Smith, *Anal. Chem.*, 62 (1990) 900.
19 H. Swerdlow and R. Gesteland, *Nucleic Acid Res.*, 18 (1990) 1415.
20 A. S. Cohen, D. R. Najarian and B. L. Karger, *J. Chromatogr.*, 516 (1990) 49.
21 H. Swerdlow, S. Wu, H. Hake and N. J. Dovichi, *J. Chromatogr.*, 502 (1990) 61.
22 L. Hernandez, R. Marquina, J. Escalona and N. A. Guzman, *J. Chromatogr.*, 502 (1990) 247.
23 R. London, *Advanc. Phys.*, 13 (1960) 423.
24 D. A. Long, *Raman Spectroscopy*, McGraw-Hill, New York, 1977, pp. 46–75.
25 C. Daniel and F. S. Wood, *Fitting Equations to Data*, Wiley-Interscience, New York, 1971.